

S-type and N-type Negative Resistances and Large-Amplitude Current Oscillations in InSb

Katsutoshi Kamakura

*Department of Electrical and Electronics Engineering
Kokushikan University
4-28-1 Setagaya, Setagaya-ku, Tokyo 154-8515, Japan
E-mail: kamakura @ kokushikan.ac.jp*

Abstract—Current-controlled negative resistance (S-type NR) and voltage-controlled negative resistance (N-type NR) have been observed in n-InSb in high electric fields in the region of avalanche breakdown under external magnetic fields at 77 K. S-type NR has been observed in n-InSb under nearly parallel electric and magnetic fields while N-type NR has been observed only in very thin samples of n-InSb under transverse magnetic fields. Large-amplitude current oscillations associated with S-type NR have been observed and the percentage of modulation $\gamma \{=(ac/dc) \times 100\}$ is 100 % at some frequencies.

I. INTRODUCTION

There have been reports on two forms of bulk negative differential resistance in a high electric field in InSb at 77 K. One is a current-controlled negative resistance (S-type NR) in the region of avalanche breakdown under an external magnetic field [1] and the other is a voltage-controlled negative resistance (N-type NR) due to Gunn effect [2]. In the previous study of S-type NR, coherent oscillations associated with S-type NR have not been reported. We have experimentally studied further detailed characteristics of S-type NR and observed coherent current and voltage oscillations associated with S-type NR by using an external resonance circuit. S-type NR has been observed under nearly parallel electric and magnetic fields. Large-amplitude current oscillations associated with S-type NR have been observed. The oscillation frequencies (0.5–22 MHz) depend strongly on the external resonance circuit. We have observed N-type NR in only thin samples of InSb whose thickness is less than about 30 μm , under the high electric field and the transverse magnetic field. In these experiments, pulsed power is used. Furthermore, by means of a dc power supply instead of pulsed power, we have observed S-type and N-type NR in very short and thin samples of n-InSb in the high electric field in the region of avalanche breakdown. S-type NR has been observed under nearly parallel electric and magnetic fields while under transverse magnetic fields, N-type NR has been

observed. We have observed RF oscillations in the samples in the region of N-type NR.

In this paper, we describe the characteristics of S-type and N-type NR and large-current oscillations in n-InSb associated with N-type NR under the application of the pulsed power. We also describe S-type and N-type NR in very short and thin samples of n-InSb under the application of the dc power.

II. EXPERIMENTAL RESULTS

In the present experiments, pulsed power with a pulse width 1 to 2.5 μsec and a repetition rate of 20 or 40 Hz was used in order to avoid heating of n-InSb samples. Figure 1 shows typical characteristics of current-controlled negative resistance (S-type NR) in two sam-

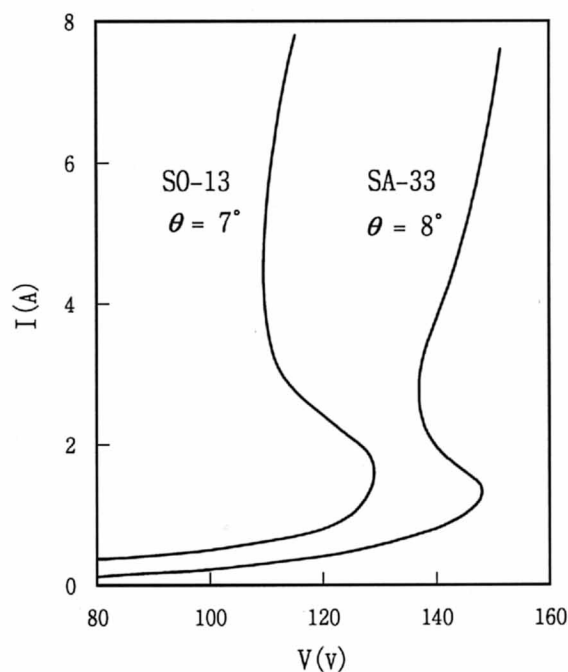


Fig. 1. Typical characteristics of current-controlled negative resistance. Applied magnetic field B_0 ; 7 kG.

ples of n-InSb at 77 K, where θ is an angle between electric and magnetic fields. The external applied magnetic field is 7 kG. Sample dimensions of SO-13 are $3.3 \times 0.7 \times 0.078$ mm and the dimensions of SA-33 are $3.7 \times 0.6 \times 0.075$ mm. In the region of negative resistances an electron-hole plasma is produced due to the impact-ionization. S-type NR has been observed above the high electric field of about 300 V/cm and the high magnetic field of about 5 kG at the angle θ between 0° and 20° .

Large-amplitude current and voltage oscillations at the frequencies from 0.5 to 22 MHz were observed in the samples of n-InSb by using the external lumped and distributed resonance circuits. Figure 2 (a) shows the distributed resonance circuit and Fig.2 (b) shows the equivalent circuit in which C is the load capacitance and L_1 and C_1 are the apparent sample inductance and capacitance, respectively. It is assumed that the apparent sample capacitance C_1 can be neglected, compared with that of the external circuit.

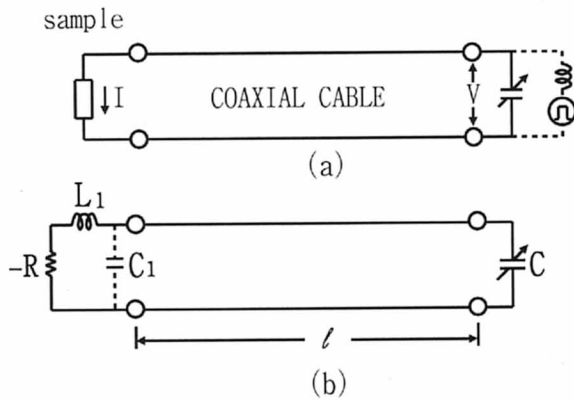


Fig. 2. Circuits of the oscillating system. (a) The distributed resonance circuit, (b) The equivalent circuit. $L_0 = 0.235 \mu\text{H}/\text{m}$, $C_0 = 94 \text{ pF}/\text{m}$, $Z_0 = 50 \Omega$.

An analysis of this circuit reveals that the resonant frequency f is given by

$$f = \frac{1}{2l(L_0 C_0)^{1/2}} \left[n + \frac{1}{\pi} \arctan\left(\frac{-\omega L_1}{Z_0}\right) - \frac{1}{\pi} \arctan\left(\frac{1}{Z_0 \omega C}\right) \right] \quad (n = 0, 1, 2, \dots), \quad (1)$$

where l is the length of the resonance line, L_0 is the inductance per unit length, C_0 is the capacitance per unit length, and Z_0 is the characteristic impedance. Oscillation frequencies were measured when the length of the resonance line was varied at $C = 0 \text{ pF}$, and the values of the load capacitance C were varied at $l = 1.2 \text{ m}$.

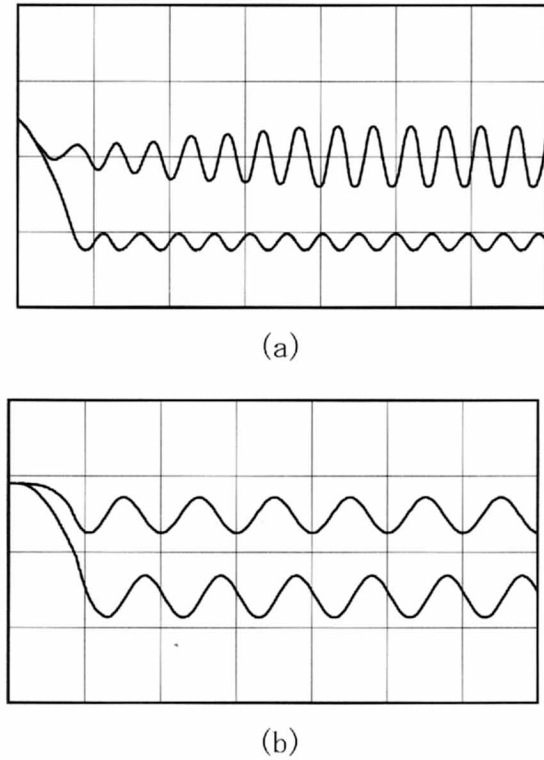


Fig. 3. Current and voltage waveforms (sample No. SA-33). Upper traces: current, 5 A/div, Lower traces: voltage, 100 V/div, Time scale, $0.1 \mu\text{sec}/\text{div}$. Applied average voltage, 143 V; sample average current, 1.8 A; applied magnetic field, 7 kG; $\theta = 8^\circ$; $l = 1.2 \text{ m}$. (a) 22 MHz, $C = 0 \text{ pF}$; (b) 10 MHz, $C = 395 \text{ pF}$.

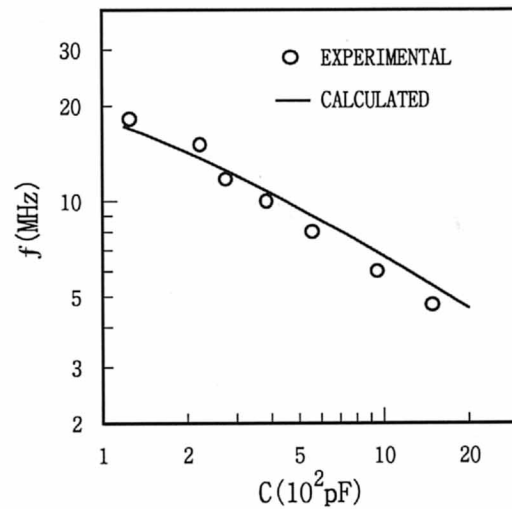


Fig. 4. Relation between the oscillation frequency f and the load capacitance C . $l = 1.2 \text{ m}$.

Figure 3 shows the oscilloscope traces of the current and voltage oscillations observed with the external distributed circuit. The current and voltage waveforms were observed at the point indicated in Fig.2 (a). It is noted that large-amplitude current oscillations are observed, for instance, when the average current (dc current) through the sample is 1.8 A, the amplitude of ac current is also 1.8 A at the frequency of 22 MHz as shown in Fig.3 (a). The calculated and observed oscillation frequencies are shown in Fig.4. The value of the apparent sample inductance ($L_1 = 0.20 \mu\text{H}$) was calculated by inserting $n = 0$, $l = 2.65 \text{ m}$, $C = 0 \text{ pF}$, and f (observed frequency) = 15 MHz into Eq.(1). It is found that observed frequencies are almost agreement with the first resonant frequencies of the external circuit with the apparent sample inductance included.

The relation between the percentage of modulation γ $\{=(ac/dc) \times 100\%$ $\}$ and oscillation frequencies is shown in Fig.5. It is found that the percentage of modulation for current is larger than that for voltage. The percentage of modulation for current becomes 100 % at the frequency of 22 MHz mentioned above.

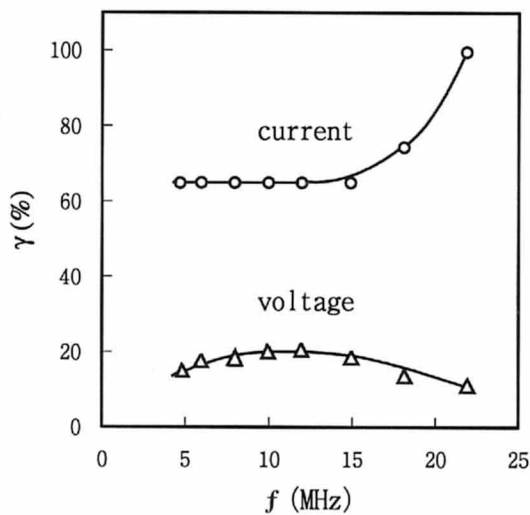


Fig. 5. Relation between the oscillation frequency f and the percentage modulation γ .

Voltage-controlled negative resistance (N-type NR) has been observed in thin samples of n-InSb above the electric field of about 600 V/cm and the transverse magnetic field of about 2 kG. Figure 6 shows characteristics of voltage-controlled negative resistance as a parameter of transverse magnetic fields. N-type NR has been observed in only thin samples of n-InSb whose thickness is less than about 30 μm . It is noted that in the thick samples showed the property of S-type NR as shown in Fig.1, N-type-NR has not been observed.

There had been reports on experimental analyses of voltage-current characteristics in InSb in a high electric field in the region of avalanche breakdown. In those experiments, the pulsed power supply was usually used.

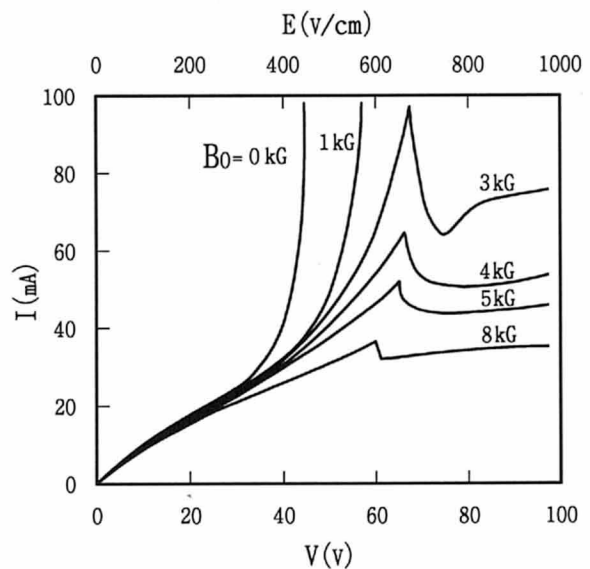


Fig. 6. Characteristics of voltage-controlled negative resistance in the thin sample under transverse magnetic fields B_0 . Sample dimensions; $1.02 \times 0.15 \times 0.008 \text{ mm}$.

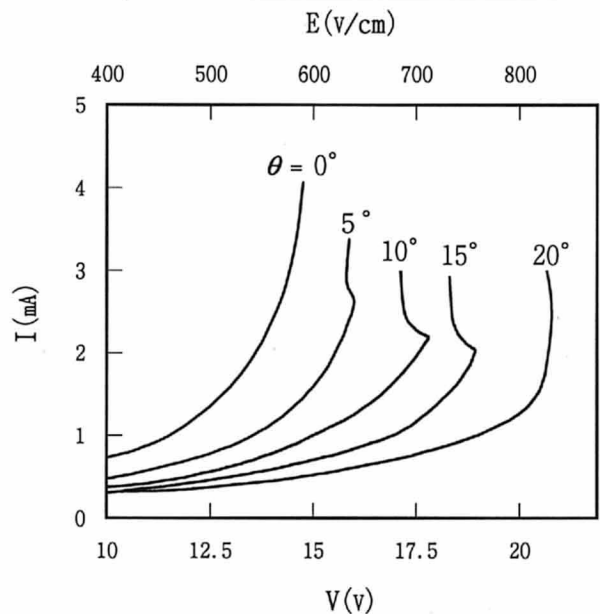


Fig. 7. Characteristics of current-controlled negative resistance in the short and thin sample under nearly parallel electric and magnetic fields. Applied magnetic field B_0 ; 8 kG.

We have observed S-type and N-type NR in very short and thin samples of n-InSb in the high electric field in the region of avalanche breakdown by means of a dc power supply instead of pulsed power. For example, the sample dimensions are $0.25 \times 0.05 \times 0.025$ mm.

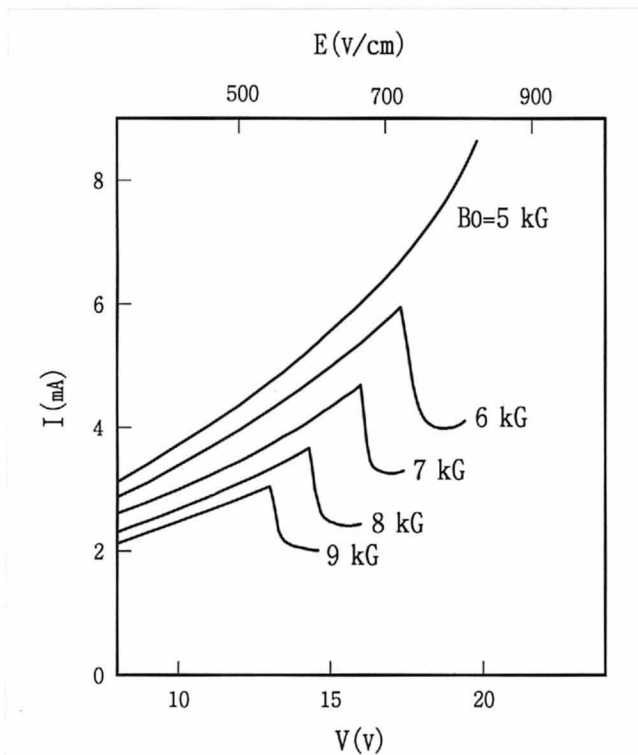


Fig. 8. Characteristics of voltage-controlled negative resistance in the short and thin sample under transverse magnetic fields B_0 .

The samples were mounted on a sapphire substrate, which was used as a heat sink, in order to avoid heating of the samples. S-type NR is observed above the electric field of about 640 V/cm and the magnetic field of about 5 kG under nearly parallel electric and magnetic fields ($\theta = 5^\circ - 15^\circ$) as shown in Fig.7. N-type NR is observed above the electric field of about 730 V/cm and the transverse magnetic field of about 6 kG ($\theta = 90^\circ$) as shown in Fig.8. We have also observed RF oscillations in the samples in the region of N-type NR by using the external resonance circuit.

III. DISCUSSION

It is noted that large-amplitude current oscillations are observed as shown in Fig.3 (a) ($\gamma = 100\%$). The observed frequencies are almost agreement with the resonant frequencies of the external circuit. In order to obtain precise theoretical oscillation frequency the nonlinear effects should be included in the analysis

since the current-voltage characteristics have a non-linear behavior. Current and voltage oscillations in InSb are due to S-type NR, however, the mechanism of S-type NR is still obscure. The negative resistance has been observed in the high electric field in the region of impact ionization. In this region the electron-hole plasma is produced. It would seem that the mechanism might be related to the helical instability in solid state plasmas [3]. There have been reports on N-type NR due to Guun effect in InSb above a high electric field of 600 V/cm [2]. N-type NR due to Guun effect in InSb exists for times less than a few nsec after the application of the electric pulse, because the avalanche breakdown in the bulk sample together with the strong avalanching in the high-field domain limits the Guun effect to the first few nsec. In the present measurements of N-type NR, pulsed power with a pulse width of 2 μ sec was used, therefore, the mechanism of N-type NR is different from Guun effect. The mechanism of N-type NR seems to be related to the two-stream instability in solid state plasmas [4], although no firm conclusion can be drawn at this stage. The mechanisms of S-type and N-type NR in the short and thin samples seem to be identical to those of negative resistances in InSb by means of the pulsed power.

IV. CONCLUSION

We have experimentally clarified S-type and N-type NR in n-InSb under the external magnetic fields by means of pulsed power supply and also clarified large-amplitude current and voltage oscillations associated with S-type NR. The observed oscillation frequencies are almost agreement with the resonant frequencies of the external circuit. In the case of very short and thin samples of n-InSb, S-type and N-type NR have been observed by means of a dc power supply.

References

- [1] K. Ando, "Transport Phenomena in InSb at High Electric and High Magnetic Fields," J. Phys. Soc. Jpn., Vol. 21, No. 7, pp. 1295-1300, 1966.
- [2] J. E. Smith, Jr., M. I. Nathan, J. C. McGroddy, S. A. Porowski, and W. Paul, "Guun Effect in n-type InSb," Appl. Phys. Lett., Vol. 15, No. 8, pp. 242-245, 1969.
- [3] M. Glicksman, "Instabilities of a Cylindrical Electron-Hole Plasma in a Magnetic Field," Phys. Rev., Vol. 124, No. 6, pp. 1655-1664, 1961.
- [4] B. B. Robinson, "Electron-Hole Plasma Instabilities," IEEE Trans. Electron Devices, Vol. ED-17, No. 3, pp. 200-206, 1970.